the aperture distribution, which showed that the maximum field strength for a given input power was the same for both antennas. The modification in radiation pattern was considerably less, however, for the short antenna.

Conclusions

Over the range of peak powers and pulse repetition rates considered here, several important conclusions may be drawn regarding the operation of traveling-wave slot antennas under breakdown conditions:

1) When breakdown occurs, the power radiated on the main lobe is essentially dependent on the peak power only.
2) For an amount of power that produces large overvoltage conditions, breakdown will occur on the leading edge of the applied pulse, and power radiated on the main lobe is constant and becomes independent of the peak power applied.
3) When large powers must be employed, it is advisable to include load isolators in the system because of the large reflection present during breakdown.
4) In the design of systems that must operate at altitudes where breakdown is likely to occur, wherever possible the peak power should be kept below the minimum breakdown potential, since the decrease in power radiated and the modification of pulse shapes are quite severe when breakdown occurs. The altitude range over which the breakdown condition exists also increases as the power is increased. For the same average power some increase in power-handling capacity may be obtained by decreasing the pulse width and increasing the pulse rate.

It should be remembered that the complex environment surrounding high-speed vehicles (air turbulence, high temperature, and excess ionization due to rocket flame and aerodynamic heating) may considerably alter the final results from those obtained in a static test. Methods for simulating some of these environmental conditions are now being considered.

Acknowledgment

The authors wish to express their appreciation to C. C. Allen and P. P. Keenan of the General Electric General Engineering Laboratory and Dr. Robert L. Tanner of Stanford Research Institute for their helpful discussions and assistance.

Some Broad-Band Transformers*

C. L. RUTHROFF†, MEMBER, IRE

Summary—**Several transmission line transformers are described which have bandwidth ratios as high as 20,000:1 in the frequency range of a few tens of kilocycles to over a thousand megacycles. Experimental data are presented on both transformers and hybrid circuits.**

Typical applications are: interstage transformers for broad-band amplifiers; baluns for driving balanced antennas and broad-band oscilloscopes; and hybrids for use in pulse reflectometers, balanced modulators, etc.

These transformers can be made quite small. Excellent transformers have been made using ferrite toroids having an outside diameter of 0.080 inch.

SEVERAL transmission line transformers having bandwidths of several hundred megacycles are described here. The transformers are shown in Figs. 1–9. When drawn in the transmission line form, the transforming properties are sometimes difficult to see. For this reason, a more conventional form is shown with the transmission line form. Some winding arrangements are also shown. Certain of these configurations have been discussed elsewhere and are included here for the sake of completeness [1–4].

In conventional transformers the interwinding capacity resonates with the leakage inductance producing a loss peak. This mechanism limits the high frequency response. In transmission line transformers, the coils are so arranged that the interwinding capacity is a component of the characteristic impedance of the line, and as such forms no resonances which seriously limit the bandwidth. Also, for this reason, the windings can be spaced closely together maintaining good coupling. The net result is that transformers can be built this way which have good high frequency response. In all of the transformers for which experimental data are presented, the transmission lines take the form of twisted pairs. In some configurations the high frequency response is determined by the length of the windings and while any type of transmission line can be used in principle, it is

* Original manuscript received by the IRE, February 5, 1959; revised manuscript received, April 1, 1959.
† Bell Telephone Labs., Inc., Holmdel, N. J.

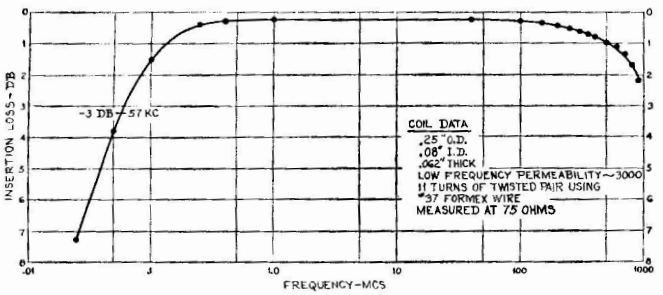

Fig. 10—1:1 Reversing transformer. Insertion loss vs frequency.

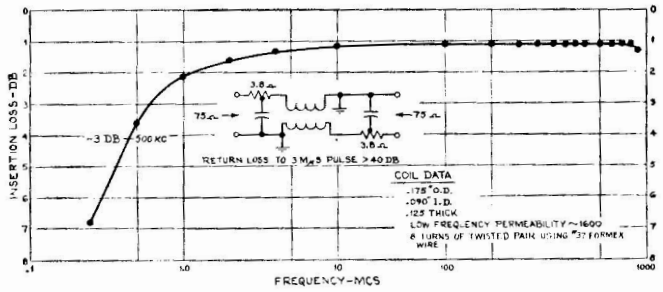

Fig. 11—Matched reversing transformer. Insertion loss vs frequency.

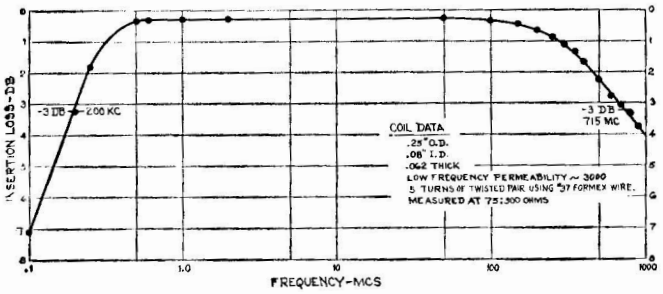

Fig. 12—1 Winding 4:1 impedance transformer unbalanced—unsymmetrical.

where β is the phase constant of the line, and l is the length of the line. Thus, the response is down 1 db when the line length is $\lambda/4$ wavelengths and the response is zero at $\lambda/2$. For wideband response this transformer must be made small. For a plot of (1) see Fig. 16.

Experimental data are given for a transformer of this type in Fig. 12.

Unbalanced-Symmetrical 4:1 Impedance Transformer—Fig. 4

This configuration requires three bifilar windings as shown in Fig. 4. All three windings can be placed on one core, a procedure which improves the low frequency response.[1] When winding multiwinding transformers the following well-known rule should be followed: with the generator connected and the load open, a completed circuit should be formed by the windings so that the core will be magnetized. The fields set up by the currents should be arranged so as to aid each other.

[1] Pointed out to the author by N. J. Pierce of Bell Telephone Labs., Inc., Holmdel, N. J.

Balanced-to-Unbalanced 4:1 Impedance Transformers—Fig. 5

The circuit of Fig. 5 is quite simple. The single bifilar winding is used as a reversing transformer as in Fig. 1. The high frequency cutoff is the same as that for the transformer of Fig. 3.

In some applications it is desirable to omit the physical ground on the balanced end. In such cases, Fig. 5(b) can be used. The high frequency cutoff is the same as for the transformer of Fig. 3. The low frequency analysis is presented in Appendix B.

Hybrid Circuits: Figs. 6–9

Various hybrid circuits are developed from the basic form using the transformers discussed previously. The drawings are very nearly self-explanatory. In all hybrids in which all four arms are single-ended, it has been found necessary to use two cores in order to get proper magnetizing currents.

Two hybrids have been measured and data included here. The response of a hybrid of the type shown in Fig. 8 is given in Fig. 13. For this measurement $R=150$ ohms. In order to measure the hybrid in a 75-ohm circuit, arms B, D were measured with 75-ohm series resistances in series with the 75-ohm measuring gear. This accounts for 3 db of the loss. Under these conditions arms B and D have a 6 db return loss.

The transmission of the resistance hybrid of Fig. 9 is given in Fig. 14. This hybrid has been matched using the technique described previously for the reversing transformer. The results of this matching are included in the figure. This hybrid was designed for use in a pulse reflectometer, the main part of which is a stroboscopic oscilloscope with a resolution of better than 3 mμsec. The oscilloscope was designed by W. M. Goodall.

Applications

Many applications for these transformers will occur to the reader. For purposes of illustration, a few of them are listed here.

1) The reversing transformer of Fig. 1 can be used to reverse the polarity of short pulses, an operation which is frequently necessary. It has also been used in balanced detectors and to drive push-pull amplifiers from single-ended generators.
2) The transformers of Figs. 2 and 5(b) are useful for driving balanced antennas. The circuit of Fig. 5(b) may find application in connecting twin lead transmission line to commercial television receivers.
3) The transformer of Fig. 3 has found wide use in broadband amplifier interstages. It will also be useful in transforming the high output impedances of distributed amplifiers to coaxial cable impedances. They can also be cascaded to get higher turns ratios.

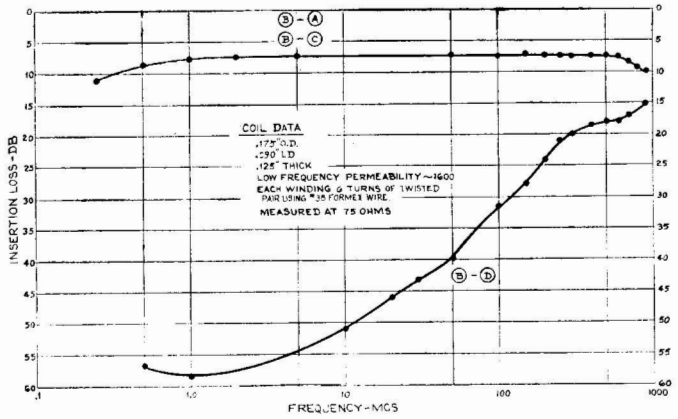

Fig. 13—Hybrid of Fig. 8. Insertion loss vs frequency.

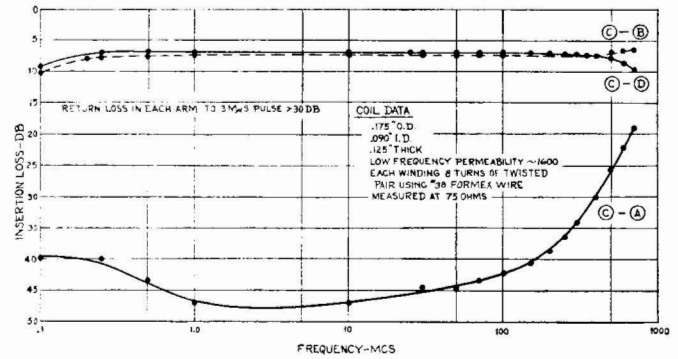

Fig. 14—Matched resistance hybrid. Insertion loss vs frequency.

4) The circuit of Fig. 5(a) has been used to drive broadband oscilloscopes, with balanced inputs, from single-ended generators. It can also find use in balanced detectors.
5) Hybrids have many uses such as in power dividers, balanced amplitude and phase detectors; as directional couplers for pulse reflectometers, IF and broadband sweepers. They might also be used as necessary components in a short pulse repeater for passing pulses in both directions on a single transmission line.

Appendix A

The high frequency response of the circuit of Fig. 3 is derived from Fig. 15. The loop equations are as follows:

$$e = (I_1 + I_2)Rg + V_1$$
$$e = (I_1 + I_2)Rg - V_2 + I_2R_L$$
$$V_1 = V_2 \cos \beta l + jI_2Z_0 \sin \beta l$$
$$I_1 = I_2 \cos \beta l + j\frac{V_2}{Z_0} \sin \beta l. \quad (2)$$

This set of equations is solved for the output power P_0. $P_0 = |I_2|^2 R_L$

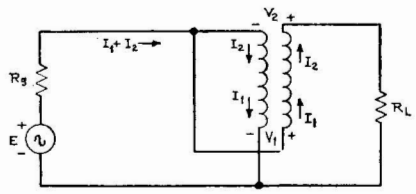

CHARACTERISTIC IMPEDANCE OF BIFILAR WINDING $=Z_0$
THE REACTANCE OF THE WINDINGS $X >> R_L, R_g$

Fig. 15—Transformer schematic.

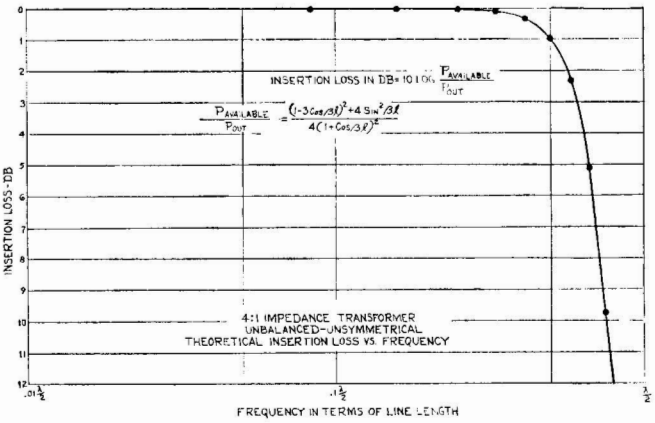

Fig. 16—Theoretical insertion loss vs frequency.

From this expression, the conditions for maximum power transmission are obtained by setting $l=0$ and setting $dP_0/dR_L\big|_{l=0}=0$. The transformer is matched when $R_L=4Rg$. The optimum value for Z_0 is obtained by minimizing the coefficient of $\sin^2 \beta l$ in (3). In this manner the proper value for Z_0 is found to be $Z_0=2Rg$.

Now, setting $R_L=4Rg$ and $Z_0=2Rg$, (3) reduces to

$$P_0 = \frac{e^2(1 + \cos \beta l)^2}{Rg[(1 + 3 \cos \beta l)^2 + 4 \sin^2 \beta l]}. \quad (4)$$

Also,

$$P_{\text{available}} = \frac{e^2}{4Rg}, \quad (5)$$

and dividing (4) by (3):

$$\frac{\text{Power Available}}{\text{Power Output}} = \frac{(1 + 3 \cos \beta l)^2 + 4 \sin^2 \beta l}{4(1 + \cos \beta l)^2}. \quad (6)$$

This function is plotted in Fig. 16.

The impedances seen at either end of the transformer with the other end terminated in Z_L have been derived. They are:

Z_{in}(low impedance end)

$$= Z_0\left(\frac{Z_L \cos \beta l + jZ_0 \sin \beta l}{2Z_0(1 + \cos \beta l) + jZ_L \sin \beta l}\right) \quad (7)$$

$$P_0 = |I_2|^2 R_L = \frac{e^2(1 + \cos \beta l)^2 R_L}{[+2Rg(1 + \cos \beta l) + R_L \cos \beta l]^2 + \left[\frac{RgR_L + Z_0^2}{Z_0}\right]^2 \sin^2 \beta l}. \quad (3)$$

and

$$Z_{in}(\text{high impedance end}) = Z_0\left(\frac{2Z_L(1+\cos\beta l)+jZ_0\sin\beta l}{Z_0\cos\beta l+jZ_L\sin\beta l}\right). \quad (8)$$

Appendix B

In the low frequency analysis of the transformer of Fig. 5 the series impedance of each half of the bifilar winding is denoted by Z. The loop equations are:

$$E=(Rg+Z)I_1-(Z+kZ)I_2$$
$$E=(Rg-kZ)I_1+(R_L+Z+kZ)I_2, \quad (9)$$

from which

$$\frac{I_1}{I_2}=\frac{R_L+2Z(1+k)}{Z(1+k)}\approx 2 \text{ if } Z\gg R_L. \quad (10)$$

We now proceed to calculate the voltages from points 1 and 2 to ground

$$V_{2G}=E=I_1Rg.$$

When the transformer is matched, $E=2I_1Rg$ and

$$V_{2G}=I_1Rg. \quad (11)$$

Similarly,

$$V_{1G}=I_2Z-kZ(I_1-I_2).$$

With the aid of (10) this can be rearranged to

$$V_{1G}=ZI_1\left[\frac{Z(1+k)^2-kR_L-2kZ(1+k)}{R_L+2Z(1+k)}\right]. \quad (12)$$

Now let the coupling coefficient $k=1$, then

$$V_{1G}=I_1Z\left[\frac{-kR_L}{R_L+2Z(1+k)}\right]\approx-\frac{I_1R_L}{4}$$

for $Z\gg R_L$.

When the transformer is matched, $R_L=4Rg$ so that

$$V_{1G}=I_1Rg=-V_{2G}, \quad (13)$$

and the load is balanced with respect to ground.

From (13) it is clear that the center point of R_L is at ground potential. This point can therefore be grounded physically, resulting in Fig. 5(a).

Acknowledgment

In addition to those mentioned in the text, the author is indebted to D. H. Ring for many stimulating discussions on every aspect of these transformers.

References

[1] Willmor K. Roberts, "A new wide-band balun," Proc. IRE, vol. 45, pp. 1628–1631; December, 1957.
[2] H. Gunther Rudenberg, "The distributed transformer," Raytheon Mfg. Co., Waltham, Mass.
[3] G. Guanella, "New method of impedance matching in radio frequency circuits," *Brown-Boveri Rev.*, vol. 31, p. 327; 1944.
[4] A. I. Talkin and J. V. Cuneo, "Wide-band balun transformer," *Review of Sci. Inst.*, vol. 28, No. 10, pp. 808–815; October, 1957.
[5] C. A. Burrus, unpublished memorandum.

Dissipation Loss in Multiple-Coupled-Resonator Filters*

SEYMOUR B. COHN†, SENIOR MEMBER, IRE

Summary—**This paper examines the effect of dissipation on the response of multiple-coupled-resonator filters designed from lossless prototype low-pass filters. A simple approximate formula makes possible the computation of center-frequency loss in terms of bandwidth, unloaded Q of the resonators, and the parameters of the prototype filter. It is shown how the insertion loss elsewhere in the pass band and stop band may be computed from the prototype filter after modifying its circuit to take account of dissipation in the resonators. The computational techniques are used to compare several symmetrical designs with each other and with unsymmetrical designs having exact maximally-flat and equal-ripple response in the presence of dissipation. It is found that the symmetrical designs offer lower pass-band loss than the unsymmetrical designs. It is proven that a symmetrical filter based on an equal-element prototype has minimum-possible center-frequency loss for given unloaded Q and stop-band bandwidth, subject to assumptions that the loss per resonator is small and that the stop-band insertion loss may be determined accurately from the highest-power term of the insertion-loss polynomial.**

* Original manuscript received by the IRE, March 2, 1959; revised manuscript received, April 20, 1959. The work described in this paper was supported by the U. S. Army Signal Res. and Dev. Lab. under Contract DA 36-039 SC-74862.
† Stanford Research Institute, Menlo Park, Calif.